PHOTOCATALYTIC DEGRADATION OF DIRECT BLUE-1 DYE ON ZrO$_2$, SULPHATED ZrO$_2$ AND V$_2$O$_5$-ZrO$_2$/SO$_4$ CATALYSTS

IBRAHEEM OTHMAN ALI[a], ABUDELRHMAN FARAG A. MOHMED[b] and MOHMED S. THABET[a]

[a]*Faculty of Science, Chemistry Department, Al-Azhar University, Nasr City 11884, Cairo, Egypt*
[b]*Faculty of Science, Chemistry Department, Sebha University, Sebh City, Libya*

Abstract

Sulfated (5wt.%) ZrO$_2$ and non-sulfated ZrO$_2$ modified by NH$_4$VO$_3$ using incipient wetness impregnation technique to achieve a loading of 5wt.% V$_2$O$_5$ were thoroughly characterized by means of X-ray powder diffraction (XRD), Fourier-transform infrared spectroscopy, N$_2$ sorptiometry, particle size analyzer and pyridine-FT-IR that was used to investigate the acidity of the samples. Degradation of direct blue-1 (DB) dye was tested for the effectiveness of the samples. The results revealed that DB degradation was highly improved with V supported on ZrO$_2$–SO$_4$ and showed a conversion comprises of 95% after UV irradiation (emitting at 365 nm) for 60 min exceeding that of SO$_4$ free ZrO$_2$ sample (68%) obtained at the same period of illumination. This was due to the large surface area (183 m^2 g^{-1}), small crystallites size and presence of basic sites namely O$_2^-$ and OH$^-$ moieties, those take part in the reaction as additional oxidizing agents. The photocatalytic degradation of DB was found to follow first order rate kinetics. More information on the activity, surface texturing, kinetics and TOC removal were well evaluated, compared and discussed for all samples.

Keywords: Acidity; Kinetics; Photodegradation; Degradation of direct blue-1 dye; Sulfated zirconia; texturing

E-mail address: iothmana@yahoo.com. (I. Othman) Fax: +20 2 2629356.

Introduction

It has been documented that some azo dyes are toxic and even mutagenic to living organisms in aquatic environment [1,2]. The release of these colored wastewaters in the ecosystem is a dramatic source of aesthetic pollution, eutrophication and perturbation degradation. Therefore, decolorization of dye effluents using new technologies with more efficiency and less energy used has acquired increasing attention. In recent years, efforts have been devoted to the study of photochemical processes using semiconductor oxides, such as TiO$_2$, ZrO$_2$, or ZnO, in heterogeneous system [3-5].

The catalytic properties of the active vanadium oxide phase can be greatly influenced by the nature of supported oxide and its dispersion on support material. ZrO_2 is an excellent support for the synthesis of highly dispersed oxides when compared to weakly interacting supports such as SiO_2. ZrO_2 also inhibits sintering of supported oxides in the presence of water and high temperature [6]. Moreover ZrO_2 consist special characteristics such as high thermal stability, extreme hardness, acidic/basic features and stability under reducing conditions.

Using the acidic catalysts in the modern chemical industries or for the production of fine chemicals have been drawn much attention recently [7]. The liquid acid like H_2SO_4 was often used; however, there were several disadvantages like the corrosion of equipments and environmental pollution. There were more and more works for developing efficient solid acids for the replacement of H_2SO_4 application [8,9], leading to cleaning processes. Since the primary work of Arata and Hino in 1979 [10], the super acids by sulfated metal oxides have gained more attention. This is because of the thermal stability and acidity gained after sulfation process [11]. In addition, doping with anionic species such as sulphur in zirconia catalysts is greater different from that of conventional solid acids. For example, the skeletal isomerization of alkene proceeds on sulfated zirconia at room temperature, while higher temperatures are needed on conventional solid acid catalysts [12]. The results of various experiments and quantum calculations [13] suggest strong acidity, sometimes referred to as superacidity [14]. The superacidity of the sulfated zirconia has, however, been disputed in a few reports [15-20]. Different understandings of the catalysis of this material could be caused by some different physicochemical properties of the synthesized samples [21].

Concerning to the crystal phase of sulfated ZrO_2, some workers claim a necessity of a tetragonal phase for the catalytic activity for reactions that need strong acid sites. For instance, Morterra et al. [22] have been prepared several sulfate-doped ZrO_2 catalysts of different crystal phases. From their results, it is concluded that the sulfated tetragonal phase ZrO_2 is catalytically active for the isomerization of *n*-butane, no matter what the preparation route has been, whereas the sulfated monoclinic phase ZrO_2 indicated very low activity for the reaction. However, it has not been clarified well why the tetragonal phase is effective for catalytic reactions such as hydrocarbon isomerization.

The surface structure of sulfated ZrO_2 has been also studied enthusiastically in order to understand the nature of the active sites [23-25].

Thus, in the present paper, we have been focused on improving photocatalytic efficiencies of ZrO_2 by sulfate ions for the purpose of decomposing degradation of direct blue-1 dye. In addition, the activity of vanadium incorporated inside zirconia either sulfated or not will also be examined. The textural properties and the crystalline structure of the materials were studied using BET, X-ray powder diffraction (XRD) and FT-IR techniques. The acidity was measured using situ FT-IR of pyridine adsorption.

Their activity in the photocatalytic degradation of direct blue-1 (DB) dye is also reported. DB was selected, as a model for the photocatalytic degradation experiment because it is a nonvolatile and common contaminant in the industrial wastewaters.

Experimental
Reagents

The materials used were: ZrO_2 (Fluka) was utilized as a photocatalyst. Ammonium sulfate was used as sulphation source where ammonium metavanadate was used as a source of vanadium and they were A.R. grade.

Direct blue-1 dye [98%$\leq$ purity] was obtained from Merck, M.F. $C_{38}H_{24}N_6Na_4O_{16}S_4$, M.Wt.*466.35*. maximum absorbance wavelength is 608 nm; molar absorbtivity is 6309 $mol^{-1}cm^{-1}$.
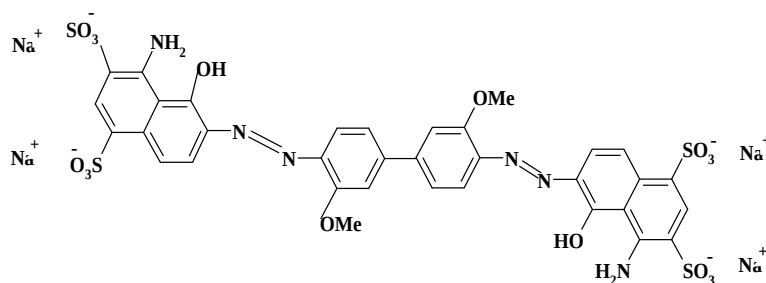
The stoichiometric equation for the degradation of DB can be written as:

$$C_{34}H_{24}N_6Na_4O_{16}S_4 + 49\,H_2O_2 \xrightarrow{\text{Catalyst}} 34\,CO_2 + 4\,SO_4^- + 6\,NO_3^- + 2\,H^+ + 4\,Na^+ + 12\,H_2O$$
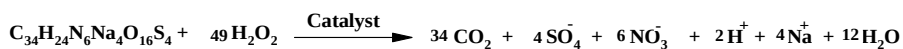
Catalyst modification
Preparation of V₂O₅/ZrO₂

Loading of V_2O_5 on ZrO_2 support was performed via incipient wetness impregnation technique. 50 ml solution of NH_4VO_3 (5wt. % V_2O_5) was vigorously stirred with small amounts of oxalic acid to improve its dissolution, the ratio of NH_4VO_3/oxalic acid was equal to 0.5 M. The solution was slowly added to 3 g of ZrO_2 with stirring at 353K for 4 h. Oxalic acid solution was evaporated at 383 K, dried at 393 K for 1 h and then calcined at 773K for 6 h in an air oven. The color after calcination was yellow.

Preparation of V_2O_5/ZrO_2–SO_4

The anchoring sulfate groups on/in zirconia sample was done by adding a definite amount of dissolved $(NH_4)_2SO_4$; to achieve 5 wt.% SO_4 on ZrO_2 support. The slurry was stirred for 2 h, drying at 393 K, and then calcined at 773K for 6 h. Vanadium containing sulfated zirconia sample was prepared as exactly mentioned above.

The color after calcinations at 773K for 6 h was dark yellow.

Characterization techniques

The X-ray diffractograms of various zirconium samples were measured by using a Philips diffractometer (type PW 3710). The patterns were run with Ni-filtered copper radiation (λ = 1.5404 Å) at 30 kV and 10mA with a scanning speed of 2θ = 2.5° min^{-1}. Identification of the phases was made with the help of the Joint committee on powder Diffraction standard (JCPDS) files. The crystallinity of the prepared samples was calculated using ratio of the sum of the areas of most intense peaks for modified ZrO_2 samples to that of the same peaks for the standard ZrO_2 and multiplying by 100.

Dynamic light scattering, LB-500, was used for determining particles size. Sample preparation was carried out as follows: dispersion of 20 mg of the sample in distilled H_2O together with sodium hexametaphosphate was stirred for 10 min. The suspension was ultrasonicated for 10 min then acquired for measurement.

The FT-IR spectra were recorded on a Bruker (Vector 22), single beam spectrometer with a resolution of 2 cm^{-1}. The samples ($20mgcm^{-2}$) were ground with KBr as a tablet and mounted to cavity of the instrument while flushing with nitrogen gas.

The nitrogen adsorption isotherms of various samples were measured at -195ºC using conventional volumetric apparatus. Prior to the determination of the adsorption isotherm, the sample (0.1g) was outgassed at 200ºC for 3h under a reduced pressure of 10^{-5} Torr in order to remove moisture. The specific surface area was obtained using the BET method while the micropore volume and the external surface area were obtained from the "*t*-plot" method.

The in situ FTIR spectra of pyridine adsorption were recorded using Bruker (Vector 22), single beam spectrometer. The sample was pressed into self-supporting wafer using 20 mg/cm^2 before being mounted between CaF_2 windows attached to a quartz infrared cell. This cell was equipped with an electric furnace for heat treatment. Prior each experiment was initiated the following procedures were carried out: (a) thermal evacuation of the sample at 573 K; (b) treatment with 16 Torr of pyridine gas at room temperature; and (c) evacuation at increasing temperatures before monitoring the IR spectrum at room temperature.

TOC (total organic carbon) analysis was conducted using a Dohrmann DC-180 carbon analyzer, which employs the low temperature UV/persulfate oxidation method [26]. Filtered samples (using PTFE syringe filters) were stored in 5ml sample vials sealed with septa, to allow measurement of dissolved inorganic carbon, without CO_2 diffusing into or out of the sample prior to analysis.

Catalytic activity

Decolorization experiments of direct blue-1 on sulfated (5 wt.%) ZrO_2 and non-sulfated ZrO_2 modified by NH_4VO_3 were carried out using a horizontal cylinder annular batch reactor. A black light-blue fluorescent bulb (F18W-BLB) was positioned at the axis of the reactor to supply UV illumination. The maximum emission of UV lamp after passing through a reaction suspension was wavelength 365 nm. A 200 ml volume of the DB-1 dye (100 ppm), previously adjusted to ffixed pH value with diluted NaOH and HCl solutions, was added into 250 ml beaker containing different amounts of suspended solids. The suspensions were immediately shaken in an air for 1 h using a magnetic stirrer prior to following up the uptaken amounts of the dye by these solids.

The reaction was carried out isothermally at 25ºC for a total reaction time 1 h. The decolorization of DB-1was analyzed at time intervals of 5 min using UV–V spectrophotometer (JASCO V-570 unit, serial no. 29635) over a range 190–800 nm. Calibration plots based on Beer's law were established relating the absorbance to the

concentration. The decolorization was determined at the maximum wavelength at 608 nm. The percentage removal efficiency of DB-1 was measured by applying the following equation:

$$\%\text{Removal efficiency} = (C_o - C)/C_o \times 100$$

where C_o is the original direct blue-1 (DB) content and C is the retained DB in solution.

Results and discussion

X-ray diffraction

X-ray diffraction patterns of $5V/ZrO_2$, $5V/ZrO_2\text{-}SO_4$ and parent ZrO_2 catalysts were shown in Fig. 1. It can be seen in Fig. 1 that all the samples showed XRD peaks due to monoclinic zirconia with major peaks at d = 3.16 and 2.834Å (JCPDS No. 37-1484). No. V_2O_5 species were developed for vanadium containing samples probably for their high dispersion at such low loadings in both samples and/or for decreasing the crystallites size of V_2O_5 to be detected by XRD technique (≤ 2 nm). The amount of vanadia needed for total coverage of support (as 2D monolayer) was estimated to be 0.145 wt% of V_2O_5 per m^2 of the support surface [27]. Therefore, ZrO_2 having surface area 127 m^2/g required a quantity of 18.4 wt% V_2O_5 to yield a single monolayer. Our results were well in agreement with the theoretical monolayer calculations. In the other hand, the crystallinity percentage of $5V/ZrO_2$ measures 96% from the ZrO_2 sample that taken as 100% crystallinity whereas $5V/ZrO_2$–SO_4 indicates 87% reflecting the effect of sulfation on this particular sample, i.e. mutual interaction between ZrO_2 and SO_4 moieties. The values of full-width-at-half maximum (FWHM) of the (d=3.16Å) peak was not much different for all zrconia samples except V/ZrO_2–SO_4 that showed little widening and hence possesses smaller crystallites size, comparatively.

Fig. 2 gives an idea about the distribution of particles size of all samples illustrating that incorporation of vanadium in ZrO_2 ($5V/ZrO_2$) exposes particles size at higher dimension from 3.61µm; in ZrO_2, to 5.32µm; in $5V/ZrO_2$. On the contrary, a narrower distribution with a mean particle size 3.32µm was rendered for $5V/ZrO_2$– SO_4 reflecting the role of sulfate groups in exhibiting the finest crystallites size among all samples.

IR spectroscopy

Fig. 3 showed the FT-IR spectra of vanadium containing zirconium samples in addition to that of the parent ZrO_2 in the frequency range of 400–1300 cm^{-1}. The latter sample showed bands at 420, 493, 578,678 and 761 cm^{-1} indicative of the ZrO_2 and characteristic of lattice vibration of Zr-O bonds. For $5V/ZrO_2$, bands at 420, 493, 578,678 and 761 cm^{-1} were depicted in addition to a small band at 1015 cm^{-1} and shoulder at 875. The band at 1015 cm^{-1} is indicative for the presence of isolated monovanadate species [5,28]. In the other hand, the wide band centered near 875cm⁻¹, assigned to V-O-V as well V-O-Zr bonding [29].
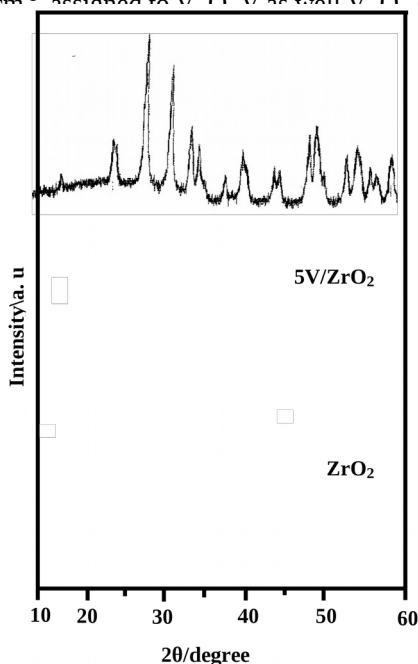

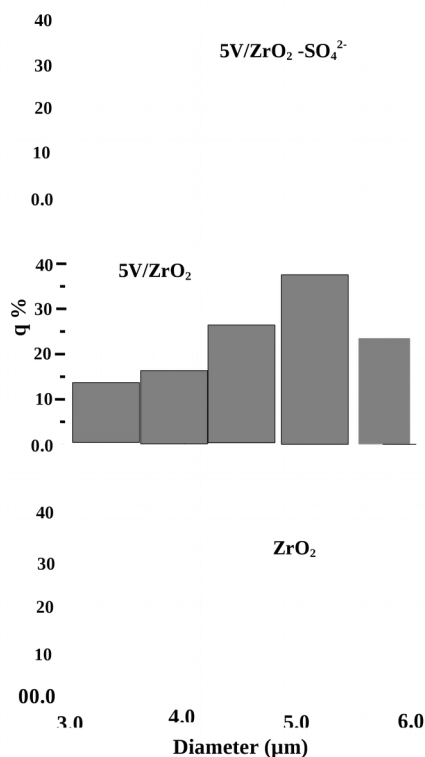Fig. 1: XRD patterns of ZrO_2, $5V/ZrO_2$ and $5V/ZrO_2$–SO_4 in comparison with V_2O_5.

Fig. 2: Particle size distribution of ZrO_2, $5V/ZrO_2$ and $5V/ZrO_2$–SO_4 samples

The spectrum of $5V/ZrO_2$–SO_4 preserved the same bands revealed for $5V/ZrO_2$ except decrease in intensities for the bands at 420, 493, 578,678 and 761cm^{-1} and 1017 cm^{-1} with the disappearance the band at 875cm^{-1} reflecting some evidence for the strong interaction between sulfate groups and zirconia particles and indicates as well a decrease in crystallinity following sulfation, as emphasized previously using

XRD investigations. The decrease in intensity of the monovanadate band at 1015 cm^{-1}; associated with V–O and disappearance the stretch band at 875cm^{-1} assigned to V–O–V or V–O–Zr bending, could be due to migration of vanadium ions into the ZrO$_2$–SO$_4$ vacant positions but more extensive tests were required to prove this definitively. This spectrum shows a broad band at 1220 cm^{-1} ascribed to the asymmetric stretching mode of S–O linkages [30] and verifying the involvement of it in the zirconia structure. From the foregoing results of XRD and IR, one can conclude the presence of SO$_4^{2-}$ in the lattice of Zr atoms probably as S^{4+} state substituting for some of the lattice Zr atoms. This was in harmony with the work of T. Ohno et al.[31] who prepared and characterized S-doped TiO$_2$ (anatase) and they suggested that the oxidation state of S is mainly as S^{4+} from XPS investigations.

Pyridine adsorption

IR spectroscopy of pyridine adsorbed on supported vanadium oxide surfaces has been examined widely in the literature [32–35], as it can be used to distinguish between the different types of surface acid sites in the catalysts. Fig. 4 shows the IR spectra of pyridine (Py) adsorbed on V/ZrO$_2$ and V/ZrO$_2$–SO$_4$ taken following out gassing at 303 K. The spectrum of Py/V/ZrO$_2$ at 300K displayed a band structure with the strongest features of which are indicative of formation of Lewis Pyridine (LPY) species, i.e. bands at 1456, 1470 and 1600 cm^{-1}. The display of a strong band at 1540 cm^{-1} due to Brønsted pyridine (BPY) let us assigned the ones at 1645 and 1650 cm^{-1} to same species but probably accounted for the involvement of two different types of Brønsted acid sites. The existence of a band at 1558 cm^{-1} is indicative for oxidative break down of LPY species into carbonaceous surface species; at such low temperature (300 K), implying the existence of considerably reactive basic sites. The latter result was confirmed also through the exposed band at 1680 cm^{-1} ascribed to vC=O of α-pyridone species [36,37].

On V/ZrO$_2$–SO$_4$, Py adsorption at 300K is shown to lead to formation of higher density LPy species comparatively, i.e. 1449, 1468 and 1603 cm^{-1} as well as BPy ones, i.e. bands at 1538, 1645 and 1660 cm^{-1}. Moreover, a medium band at 1515 cm^{-1} indicative of pyridinum oxide species was also depicted as previously envisaged by others [38]. These results have been considered [39,40] indicative of existence of reactive basic O$_2^-$ species on V/ZrO$_2$–SO$_4$ surfaces but of lower density than those delivered on 2V/ZrO$_2$. Generally, the detection of pyridinium oxide species is rather indicative of the availability of acid base pair sites. The higher the frequency assumed by the v19b mode (1456 cm^{-1}) for 5V/ZrO$_2$, the stronger the acidity of the

Lewis coordination site. Hence, the formation of Py oxidation species seems to have been preceded by conversion into α-pyridone species (vC=O band at 1680 cm^{-1}) and hence reveals existence of active nucleophilic (basic) OH groups rather than V/ZrO$_2$–SO$_4$. It can be inferred that differences in reactivity of basic sites are related to the sulfate moieties, that affect the geometric arrangement of OH$^-$ or/and O$_2$$^-$ ligands. This explains the reactivity of basic sites of V/ZrO$_2$ due to the major contribution of LPY species comparatively. This figure also shows that Brønsted acid sites, i.e. proton acidity, appeared on the sulfated sample with higher population than that on nonsulfated one.
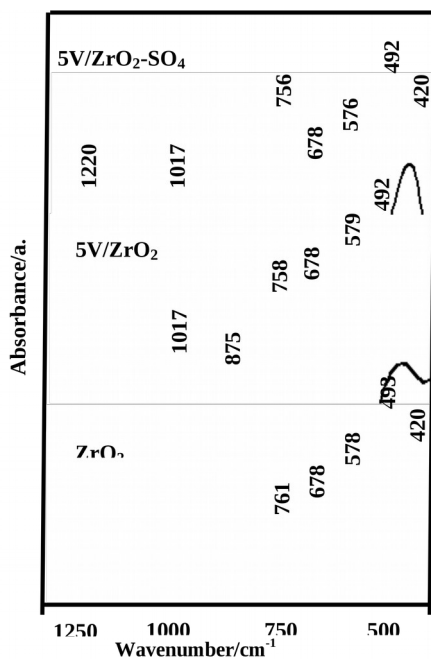
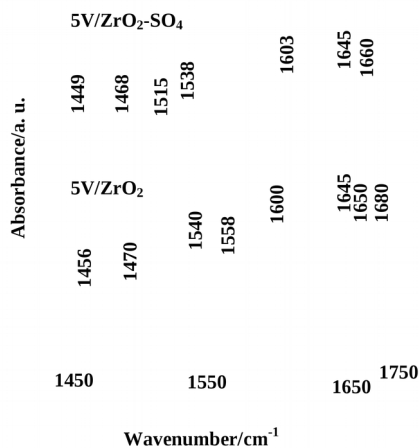Fig. 3: FT-IR spectra of ZrO₂, 5V/ZrO₂ and 5V/ZrO₂–SO₄ in the 400–1300 cm⁻¹ range.

Fig. 4: In situ FT-IR spectra in the 1400–1750 cm⁻¹ range due to pyridine adsorption at room temperature. The spectra were recorded after evacuation for 10 min at 300 K.
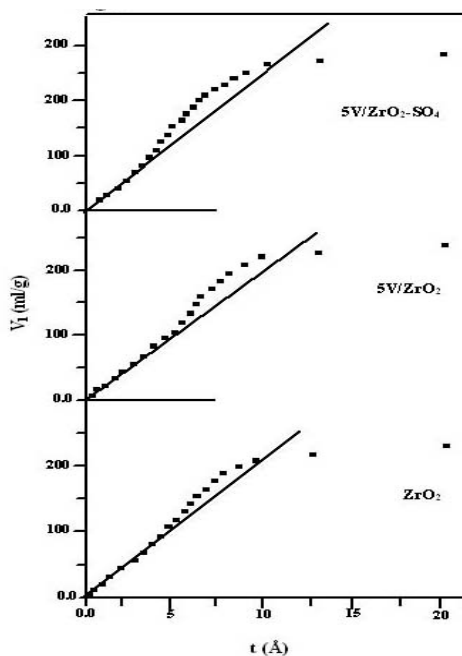
Surface texturing

The different surface characteristics of the synthesized zirconia samples were determined and the data obtained was compiled in Table 1. Inspection of this Table reveals the following: (i) the vanadium containing zirconia samples especially 5V/ZrO₂–SO₄ measured higher surface areas (44.1%) than that of the parent implying the presence of fine particles in this sample as confirmed from XRD and particles size investigations. Thus, the main reason of surface area increment is due to the retardation of crystallization of the ZrO₂ following the sulfation process. This lowering degree of crystallinity, as evidenced from XRD pattern, supports the increase in surface area via sulfate treatment. (ii) the computed values of pore radius of different samples show the dominant of mesoporosity (30–43Å). The sample designated as 5V/ZrO₂ measured maximum V_p and maximum r when compared with rest of samples indicating the enforced location of V species in the pores of this sample leading to an effective pore widening and pore volume.

Table 1: Texturing properties of V contaning sulphated and non-sulphated zrconia catalysts

Samples	S_{BET} (m²/g)	S_t (m²/g)	Vp (cm³/g)	r⁻ (Å)
ZrO_2	127	122	0.211	33.2
$5V/ZrO_2$	151	157	0.321	42.5
$5V-SO_4/ZrO_2$	183	195	0.275	30.1

V_{1-t} plots of the samples (Fig. 5), those constructed depending on the value of C-constant in the BET equation; indicate intracrystalline mesopores as illustrated from upward deviations depicted for all samples. The V_{1-t} plots obtained for $5V/ZrO_2$ and $5V/ZrO_2$–SO_4 samples show larger upward deviations (as noted in the t range 6–11.5 and 4–11.5 Å, respectively) when compared with that of the parent ZrO_2 sample (t = 5.5–10 Å) proposing wider pore radius and pore volume. Comparable swings or hysteresis loops were observed in adsorption–desorption isotherms of type IV (not shown) for former samples at relative pressures p/pº 0.45–0.9 and 0.4–0.9, respectively, indicating the presence of mesopores. A sharp adsorption step at p/pº near 0.35 is observed for all samples due to capillary condensation in mesopores.
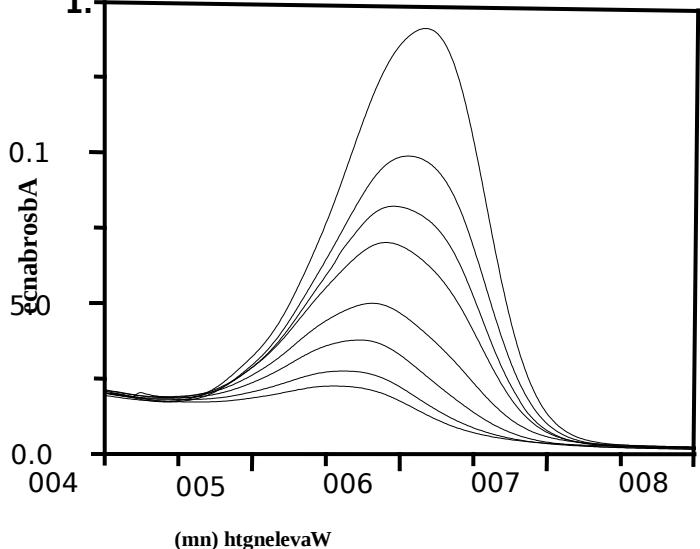

Fig. 5: V_{1-t} plots of ZrO_2, $5V/ZrO_2$ and $5V/ZrO_2$–SO_4 samples

Direct blue-1 (DB) degradation

Activity

The degradation of DB as a model reaction was studied to investigate the photocatalytic activities of $5V/ZrO_2$ and $5V/ZrO_2$–SO_4 samples under UV irradiation. The changes in the concentration of DB recorded during UV irradiation at specific time intervals were shown in Fig. 6 (a,b). Figure 6-a showed that the spectral evolution of Direct Blue-1 solution with irradiated by UV light after different time. It was observed that the absorption spectrum of the dye was characterized by a band in visible region with its maxima located at 608 nm. In general, the absorbance at 400–800 nm corresponds to the n-π* transition of the azo forms, which is due to the color of azo dyes and used to monitor the decoloration [41,42]. The absorbance at 608 nm of the dye decreased gradually with prolonging exposure time due to the increase of the decoloration and degradation. Meanwhile a shift of absorption band from 608 to 566 nm and gradually decreased. This indicated that a series of intermediates may have been formed and the whole conjugated chromophore structure of Direct Blue-1 may have been cleaved. After reaction for 1 h, a very low level of absorbance spectrum was observed. It indicated that most intermediates could have been further oxidized to lower molecule organic compounds or carbon dioxide [43].

Fig. 6-b shows that the conversion of DB with UV-light irradiation when applied on the $5V/ZrO_2$–SO_4, i.e. the conversion of DB reached 95% after 60 min UV-light irradiation. On the other hand, the $5V/ZrO_2$ catalyst shows a conversion activity approaches 80% in the same time. These results indicate the superior photocatalytic activity of $5V/ZrO_2$–SO_4 when compared with $5V/ZrO_2$, suggesting that the degradation of DB originated not only from $5V/ZrO_2$ but also from sulfate containing catalyst.

The degradation of DB on ZrO_2 (not shown) indicated, 54% decreases in the concentration. Unexpectedly, ZrO_2–SO_4 indicates a conversion comprises of 68% relatively. This demonstrates the higher solar photocatalytic activity of V/ZrO_2–SO_4 under similar conditions. This can be rationalized to surface and structural characteristics that indicated large surface area, mesoporous texture and high crystallinity.

Fig. 6-a. The time dependent UV visible
Initial concentration of D   Spectra from top to
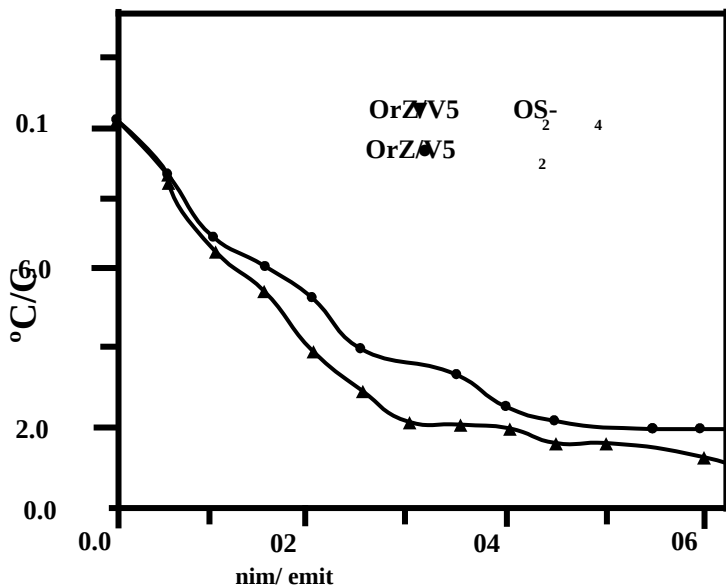bottom corresponds to irri

Fig. 6-b: Concentration of DB changes as a function of UV-irradiation time.
Conditions; C_0 = 100ppm, weight of catalyst 0.1 g, V = 200 ml.

In a way of searching on the reasons responsible for increasing the decolor rate of DB on sulfated zirconia, the adsorption course of all ZrO_2 samples; under dark conditions, was carried out. The amount of DB removed from the liquid phase containing sulfated zirconia sample was increased by time reaching to 25% and stabilized after 30 min. On the other hand, the ZrO_2 parent sample showed negligible adsorption ability whereas, $5V/ZrO_2$ induces a removal percentage comprises of 20% and stabilized after 15 min. The slight increase in DB amount adsorbed on $5V/ZrO_2–SO_4$ could be due to increasing the mesopore radius of the latter (30.1Å) that was able to incorporate DB (17.0 Å) molecules, i.e. DB molecules can diffuse freely inside the pores. This implies that increasing the pore radius intensively is not the only factor responsible for effective adsorption of DB but also the S_{BET} value that showed an incredible enhancement in $5V/ZrO_2–SO_4$.

Another driving force for the adsorption process is the increased concentration gradient between the dye in solution and on the sulfated zirconia sample. Considering the dye adsorption is the prime factor affecting the photocatalytic activity thus, the difference in the DB removal between the UV illuminated and dark conditions ((Δ(UV dark)) is used as an apparent measure to evaluate only the impact of the UV illumination on the DB removal. This indicates that the activity revealed upon exposing to UV irradiation for $5V/ZrO_2–SO_4$ (95−25 = 70%) is indicative of existing higher photodecomposition sites on its surface. In general, external mass transfer is characterized by the initial solute uptake and can be calculated from the slope of plot of C/C_0 versus time. The slope of such plots (especially in the first 10 min) can be calculated by either assuming a polynomial relation between C_t/ C_0 and time or assuming that the relationship is linear for the first points collected in 10 min. These methods were used by Fernadez et al. [44] during studying the adsorption of lauryl benzyl sulfonate on algae residue. The second method was employed in our case and the calculated sorption K_s was found to be 0.0176 and 0.01699 min^{-1} for $5V/ZrO_2–SO_4$ and $5V/ZrO_2$ catalysts, respectively, assuming that the external mass transfer occurs in the first 10 min for both catalysts in addition to the increased rate on the former, comparatively.

Kinetics

The investigation of DB kinetics in aqueous solution under UV-light irradiation is shown in Fig. 6. The degradations follow an apparent first order process. Assuming that the hydroxyl radical OH is the primary oxidant for degradation of DB, a chemical kinetics for the process may be written as

$$\text{OH} + \text{DB} \rightarrow \text{products} \qquad\qquad 1$$

That allows an expression for the reaction rate of the degradation of DB, such as

$$r = \frac{dc}{dt} = \frac{k\,K\,C}{1 + KC} \qquad\qquad 2$$

where r is the degradation rate of the reactant (mg/l min), C the concentration of the reactant (mg/l), t the illumination time, k the reaction rate constant and K is the adsorption coefficient of the reactant (l/mg). When the chemical concentration C_0 is micromolar, Eq. (2) can be simplified to an apparent first-order equation:

$$\ln (C_o/C) = k\,K\,t = Kapp \qquad\qquad 3$$

A plot of ln (C_0/C) against time represents approximately linear straight lines, showing the case of the first-order reaction. The slope of the line equals the apparent first-order rate constant K_{app}. As can be seen from the figure, the degradation rate is faster for 5V/ZrO$_2$–SO$_4$ than for 5V/ZrO$_2$. The determined K_{app} values are 0.037 min^{-1} for the former and 0.030 min^{-1} for the latter.

Fig. 7: First-order relation ln(C_0/C) = F (t). Conditions; C_0 = 100ppm, weight of catalyst 0.1 g, V = 200 ml.

IBRAHEEM OTHMAN ALI, *et al.*,

TOC measurement

The TOC measures the total amount of organic carbon in the wastewater. Therefore the decrease in the TOC represents oxidation of some of the organic material to CO_2 and thus indicates the amount of completely destructive oxidation occurring in the system. The results of TOC measurements under UV irradiation show values comprise of 90% and 73% within 60 min for $5V/ZrO_2$–SO_4 and $5V/ZrO_2$ samples (Fig.8), respectively. Since a greater TOC decay is found for $5V/ZrO_2$–SO_4 than for $5V/ZrO_2$, it is apparent that OH[*] is more efficiently generated on the former than that on the latter.

The dependence of the photodecomposition on the sulfate groups attached to Zr can be explained in view of increasing the electron accepting capacity as envisaged from increasing the Lewis acid sites density and thus a decreased in the recombination of holes and electrons is expected, i.e. long-lived OH radicals.
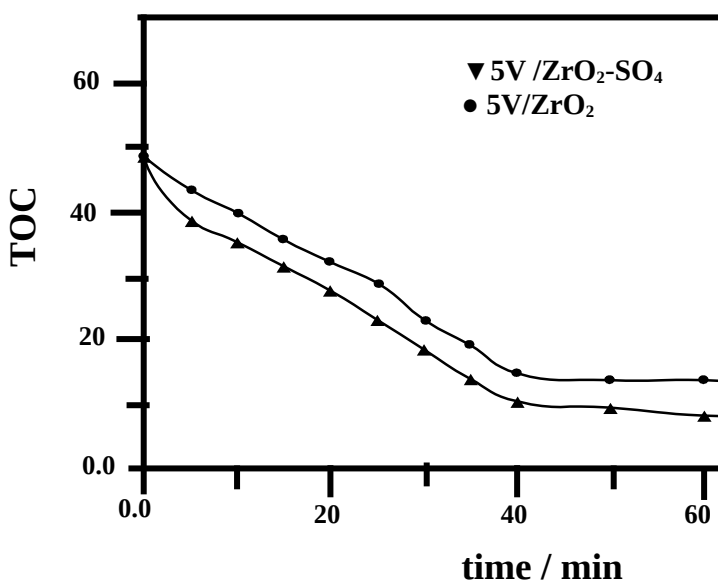

Fig. 8: Mineralization of 0.2mM DB in the presence of UV irradiation in   presence of 0.1g catalyst

Generally, one can attribute the improvement of the photocatalytic activity of metal incorporated zirconia; only at such low loadings, when compared with the neat zirconia to the increased electronegativity of V ions thus behave as an electron acceptor centers to decrease any possible recombination between holes and electrons

[45]. Another possibility of degradation of DB can be obtained through the existed reactive basic sites (O^{2-}) detected on the surface of sulfated zirconia. This can be attained by reacting the produced oxygen with photogenerated electron (e^-) leading to the generation of $O_2^{\bullet-}$ and thus preventing the recombination of e^- and h^+. $O_2^{\bullet-}$ also can degrade DB as reactive oxygen species [46,47]. However, it seems that $O_2^{\bullet-}$ is not the only active species capable for degrading DB since V/ZrO_2 owns larger amounts of such species, comparatively. This let us presume that hydroxyl radical is considered as the main oxidizing agent. On the other hand, the probability of yielded $O_2^{\bullet-}$ to react with H protons, specifically $5V/ZrO_2–SO_4$, to produce $HO_2^{\bullet}$ is most likely since sulfated zirconia acquired higher Brønsted acidity and thus $HO_2^{\bullet}$ is one of the oxidizing agents present in the reaction mixture but however of lower activity when compared with $OH^{\bullet}$ Generally, the revealed photocatalytic activity of $5V/ZrO_2–SO_4$ upon UV irradiation is most probably due to charge-transfer excited state between V species and ZrO_2 particles. An electron transfer from O_2^- to V^{5+} ions can develop $(V^{4+}–O^-)^*$ moieties, which by their turn can play a role in the enhancement of the reaction as well. The mechanism is assumed up in diagram 1.

$$OH^* + dye = \text{degradation of the dye}$$
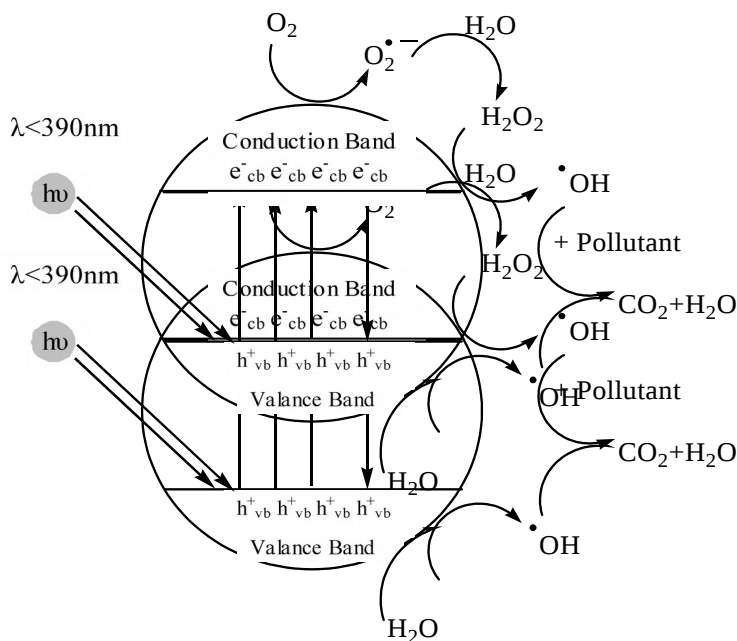
Schematic diagrams 1: The General mechanism of the photocatalysis [48,49]

Conclusions

The modification of $5V/ZrO_2$ by sulfate ions contributes to promote the photocatalytic efficiency of zirconia towards fully decomposing DB dye in 60 min reaction time; in presence of of UV lamp emitting at 365 nm, when compared with sulfate free zirconia sample indicated that:

1. The promotional effect of sulfated sample was due to the high surface area, mesopore structures, small crystallites size.

2. Appropriate basic (OH^-, O_2^-) sites in addition to the substantial amounts of Lewis acidity that owned vacant sites susceptible for more active sites.

3. Degradation of DB was 1.4 times lower on zirconia compared to $5V/ZrO_2$–SO_4.

4. The sorption process was found to be dependent mainly on external transfers at earlier stages and hence high lighting the effect of surface properties on the adsorption process and consequently on the catalytic enhancement.

5. The importance of structural and surface properties; besides the band gap energy, of the V/ZrO_2-SO_4 in exhibiting higher photocatalytic activities.

References

1. H.M. PINHEIRO, E. TOURAUD, O. THOMAS, Dyes Pigments 61 (2004) 121-139.

2. K.T. CHUNG, G.E. FULK, A.W. ANDRES, Appl. Environ. Microbiol. 42 (1981) 641-648.

3. T. SAUER, G. CESCONETO NETO, H.J. JOSE, R.F.P.M. MOREIRA, J. Photochem. Photobiol. A: Chem. 149 (2002) 147-154.

4. C.M. SO, M.Y. CHENG, J.C. YU, P.K. WONG, Chemosphere 46 (2002) 905-912.

5. M. M. MOHAMED, M. M. AL-ESAIMI, J. Molecular Catalysis A: 255 (2006) 53-61.

6. F.C. MEUNIER, A. YASMEEN, J.R.H. ROSS, Catal. Today 37 (1997) 33 42.

7. H. MATSUHASHI, T. TANAKA AND K. ARATA, J. Phys. Chem. B 105 (2001) 9669–9671.

8. K. ARATA, H. MATSUHASHI, M. HINO, H. NAKAMURA, Catal. Today 81 (2003)17-30

9. K.T. WAN, C.B. KHOUW, M.E. DAVIS, J. Catal. 158 (1996) 311-326.

10. (a) M. HINO, K. ARATA, CHEM. LETT. (1979) 12591260; (b) M. HINO, K. ARATA, Chem. Lett. (1979) 477-480; (c) M. HINO, K. ARATA, J. Chem. Soc., Chem. Commun. (1980) 851-852.

11. M.M. MOHAMED, B. ABU-ZIED, Thermochim. Acta 359 (2) (2000) 109-117; T. Okuhara, N. Mizuno, M. Misono, Appl. Catal. A: Gen. 222 (2001) 63-77.

12. H. MATSUHASHI, H. SHIBATA, H. NAKAMURA K. ARATA, Appl. Catal. A: Gen. 187 (1999)99-106.

13. T. KANOUGI, T. ATOGUCHI, S. YAO, J. Mol. Catal. A: Chem. 177 (2002) 289-298.

14. N. KATADA, J. ENDO, K. NOTSU, N. YASUNOBU, N. NAITO, M. NIWA, J. Phys. Chem. B 104 (2000) 10321-10328.

15. L.M. KUSTOV, V.B. KAZANSKY, F. FIGUERAS, D. TICHIT, J. Catal.150(1994)143-149.

16. V. ADEEVA, J.W. DEHAAN, J. JANCHEN, G.D. LEI, V. SCHUNEMANN, L.J.M. VANDEVEN, W.M.H. SACHTLER, R.A. VANSANTEN, J. Catal. 151 (1995) 364-372.

17. F. BABOU, G. COUDURIER, J.C. VEDRINE, J. Catal. 152 (1995) 341-349.

18. H. MATSUHASHI, H. NAKAMURA, T. ISHIHARA, S. IWAMOTO, Y. KAMIYA, J. KOBAYASHI, Y.KUBOTA, T. YAMADA, T. MATSUDA, K. MATSUSHITA, K. NAKAI, H.NISHIGUCHI, M. OGURA, N. OKAZAKI, S. SATOM, K. SHIMIZU, T. SHISHIDO, S.YAMAZOE, T. TAKEGUCHI, K. TOMISHIGE, H. YAMASHITA, M. NIWA, Naonobu Katada, Appl. Catal.360 (2009) 89-97.

19. T. SHISHIDO, T. TANAKA, H. Hattori, J. Catal. 172 (1997) 24-33.

20. T. SHISHIDO, H. HATTORI, J. Catal. 161 (1996) 194-197.

21. T. TATSUMI, H. MATSUHASHI, K. ARATA, Bull. Chem. Soc. Jpn. 69 (1996) 1191-1194

22. C. MORTERRA, G. CERRATO, F. PINNA, M. SIGNORETTO, J. Catal. 157 (1995)109-123.

23. L.M. KUSTOV, V.B. KAZANSKY, F. FIGUERAS, D. TICHIT, J. Catal. 150 (1994) 143-149.

24. F. BABOU, G. COUDURIER, J.C. VEDRINE, J. Catal. 152 (1995) 341-349.

25. V. ADEEVA, J.W. DE HAAN, J. JANCHEN, G.D. LEI, V.SCHUNEMANN, L.J.M. VAN DE VEN, W.M.H. SACHTLER, R.A. VAN SANTEN, J. Catal. 151 (1995) 364-372.

26. Rosemount Analytical, Dohrmann Division, Santa Clara. DC-180 Automated TOC Analyzer Opertation Manual 1989.

27. V.R.C. KOMANDUR, R. KANAPARTHI, D. NARESH, P. V. RAMANA RAO, A. RAMACHANDRA RAO, Vattikonda Venkat Rao, Catal. Today 141 (2009) 187-194.

28. B. OLTHOF, A. KHODAKOV, A.T. BELL AND E. IGLESIA, J. Phys. Chem. B 104 (2000) 1516–1528.

29. D. I. ENACHEA, E. BORDES-RICHARD, A. ENSUQUE, F. BOZON-VERDURAZ, Appl. Catal. 278 (2004) 93-102.

30. D. STOILONA, M. GEORGIEV, D. MARINOVA, Vib. Spectrosc. 39 (2005) 46-49.

31. T. OHNO, M. AKIYOSHI, T. UMEBAYASHI, K. ASAI, T. MITSUI, M. MATSUMURA, Appl. Catal: A 265 (2004) 115-121.

32. F. HATAYAMA, T. OHNO, T. MARUOKA, T. ONO, H. MIYATA, J. Chem. Soc., Faraday Trans. 87 (1991) 2629–2633.

33. T. BLASCO, A. GALLI, J.M. LṔEZ NIETO, F. TRIFIR,̄ J. Catal. 169 (1997) 203–211.

34. J. KERNEN, A. AUROUX, S. EK, L. NIINIST, Appl. Catal. A 228 (2002) 213–225.

35. J. DATKA, A.M. TUREK, J.M. JEHNG, I.E.WACHS, J. Catal. 135 (1992) 186–199.

36. I. OTHMAN ALI, Mater. Sci. and Eng. A 459 (2007) 294–302

37. M. M. MOHAMED, T.M. SALAMA, I. OTHMAN, G.A. EL-SHOBAKY, Appl. Catal. A: 279 (2005)23-33.

38. M.W. URBAN, Vibrational Spectroscopy of Molecules and Macromolecules on Surfaces,Wiley, Chichester, (1993), 171-185.

39. M.I. ZAKI, M.A. HASAN, F.A. AL-SAGHEER, L. PASUPULETY, Colloids Surf. A 190 (2001) 261-274.

40. M.I. ZAKI, G.A.M. HUSSEIN, S.A.A. MANSOUR, H.A. EL-AMMAWY, J. Mol. Catal. 51 (1989)209-220.

41. DONG, Y., HE, L., & YANG, M. Dyes and Pigments, 77(2) (2008)343–350.

42. I. OTHMAN, R.M. MOHAMED, I.A. IBRAHIM, M. M. MOHAMED, Appl. Catal. A: 299   (2006) 95–102.

43. YA-LI SONG & JI-TAI LI & BO B, Water Air Soil Pollut 213(2010)311–317

44. N.A. FERNADEZ, E. CHACIN, E. GUTIERREZ, N. ALASTRE, B. LLAMOZA, C. F. FORSTER, Bioresour. Technol. 54 (1995) 111-115.

45. K.R. SUNAJADEVI, S. Sugunan, Catal. Commun. 6 (2005) 611-616.

46. Y. YANG, G.YIHANG, H. CHANGWEN, W. YUANHONG, E. WANG, APPL. CATAL A: Gen.273(2004) 201-210.

47. Y. GUO, C. HU, C. JIANG, Y. YANG, S. JIANG, X. LI, E. WANG, J. Catal. 217 (2003) 141-151

48. N. DANESHVAR, D. SALARI, A. R. KHATAEE. J. Photochem. Photobiol. A: Chemistry. 162, (2004) 317-322.

49. C. GALINDO, P. JACQUES, A. KALT, J. Photochem. Photobiol. A: 130 (2002) 35.